ISSN 1063-7788, Physics of Atomic Nuclei, 2014, Vol. 77, No. 5, pp. 613–622. © Pleiades Publishing, Ltd., 2014.

ELEMENTARY PARTICLES AND FIELDS
Experiment

Centrality Dependence of Rapidity Spectra of Negative Pions in ^{12}C+^{12}C and ^{12}C+^{181}Ta Collisions at 4.2 GeV/c Per Nucleon*

Kh. K. Olimov[1),2)], Sayyed A. Hadi[3)], and Mahnaz Q. Haseeb[1)]*****

Received July 19, 2013

Abstract—The centrality dependences of the experimental rapidity as well as transverse momentum versus rapidity spectra of negative pions were analyzed quantitatively in ^{12}C+^{12}C and ^{12}C+^{181}Ta collisions at 4.2 GeV/c per nucleon using fitting the pion spectra by Gaussian distribution function. The experimental results were compared systematically with the predictions of the Quark–Gluon–String Model (QGSM) adapted to intermediate energies.

DOI: 10.1134/S1063778814050159

INTRODUCTION

A large number of pions are produced in relativistic hadron–nucleus and nucleus–nucleus collisions. Therefore these pions may carry important information on dynamics of a nuclear collision. It should be mentioned that the negatively charged pions can be unambiguously separated from the other particles produced in nuclear collisions. The pions are the particles produced predominantly at the energies of Dubna synchrophasotron. Production of a large fraction of pions in hadron–nucleus and nucleus–nucleus collisions at the energies of the order of few GeV/nucleon was shown to be due to excitation of baryon resonances, which finally decay into nucleons and pions. In [1–9] it was estimated that the significant fraction of pions produced in bubble chamber experiments of Joint Institute for Nuclear Research (JINR, Dubna, Russia) came from decay of Δ resonances.

The rapidity distributions of pions in relativistic nuclear collisions were studied earlier in [10–13]. The momentum, transverse momentum, and rapidity distributions of negative pions produced in Mg + Mg collisions at 4.3 GeV/c per nucleon were analyzed in [13]. It was observed [13] that the rapidity distributions of pions followed a Gaussian shape. Analysis of pion rapidity distribution showed that the central rapidity region was occupied with pions of larger transverse momentum as compared to the fragmentation region of interacting nuclei. The experimental results could be described satisfactorily by the Quark–Gluon–String Model (QGSM) [14–17]. The rapidity distributions of negative pions in (p, d, α, C)C and (d, α, C)Ta collisions at 4.2 GeV/c per nucleon were analyzed in various intervals of transverse momentum of π^- mesons in [11, 12]. With increasing the transverse momentum of negative pions, the fraction of π^- mesons in the central rapidity region increased, whereas the corresponding fraction in the fragmentation region of colliding nuclei decreased [11, 12]. The centrality dependence of pion rapidity spectra in minimum bias ^{12}C+^{12}C and ^{12}C+^{181}Ta collisions at a momentum of 4.2 GeV/c per nucleon was partly studied in early work [10] on statistics of 7900 ^{12}C+^{12}C and 2000 ^{12}C+^{181}Ta collision events. It was shown [10] that the pion rapidity spectrum was Gaussian in shape regardless of the target mass number and collision centrality. The QGSM could reproduce quite satisfactorily the main features of pion rapidity as well as transverse momentum spectra [10].

This work is a continuation of our recent papers [18, 19] devoted to analysis of various characteristics of negative pions produced in nucleus–nucleus collisions at 4.2 GeV/c per nucleon. The aim of this work is to study the dependences of experimental rapidity distributions of negative pions produced in ^{12}C+^{12}C and ^{12}C+^{181}Ta collisions at a momentum of 4.2 GeV/c per nucleon on the mass of target nucleus and collision centrality. Also the dependence of the transverse-momentum-versus-rapidity spectra of negative pions on the mass of target nucleus and collision centrality will be investigated. In order to

*The text was submitted by the authors in English.

[1)]Department of Physics, COMSATS Institute of Information Technology, Islamabad, Pakistan.
[2)]Physical–Technical Institute of SPA "Physics–Sun" of Uzbek Academy of Sciences, Tashkent.
[3)]Karakoram International University, Gilgit-Baltistan, Pakistan.
**E-mail: olimov@comsats.edu.pk
***E-mail: mahnazhaseeb@comsats.edu.pk

Table 1. Mean multiplicities per event of negative pions and participant protons and the average values of rapidity and transverse momentum of π^- mesons in $^{12}C+^{12}C$ and $^{12}C+^{181}Ta$ collisions at 4.2 GeV/c per nucleon. (The mean rapidities are calculated in cms of nucleon–nucleon collisions at 4.2 GeV/c.)

Type		$\langle n(\pi^-)\rangle$	$\langle n_{\text{part.prot}}\rangle$	$\langle y_{\text{cm}}\rangle$	$\langle p_t(\pi^-)\rangle$, GeV/$c$
$^{12}C+^{12}C$	Exper.	1.45 ± 0.01	4.35 ± 0.02	-0.016 ± 0.005	0.242 ± 0.001
	QGSM	1.59 ± 0.01	4.00 ± 0.02	0.007 ± 0.005	0.219 ± 0.001
$^{12}C+^{181}Ta$	Exper.	3.50 ± 0.10	13.3 ± 0.2	-0.34 ± 0.01	0.217 ± 0.002
	QGSM	5.16 ± 0.09	14.4 ± 0.2	-0.38 ± 0.01	0.191 ± 0.001

perform quantitative analysis, the widths and centers of rapidity as well as the $\langle p_t\rangle$ versus y_{cm} spectra of negative pions in $^{12}C+^{12}C$ and $^{12}C+^{181}Ta$ collisions will be extracted from fitting these spectra with Gaussian distribution function. The experimental results will be compared systematically with the corresponding results calculated using QGSM [14–17].

In the present work, we use QGSM developed to describe hadron–nucleus and nucleus–nucleus collisions at intermediate and relativistic energies [14–17]. In the QGSM, hadron production takes place via formation and decay of quark gluon strings. In the present analysis, we use the version of QGSM [15] adapted to the range of intermediate energies ($\sqrt{s_{nn}} \leqslant 4$ GeV). The incident momentum of 4.2 GeV/c per nucleon for the collisions analyzed in the present paper corresponds to incident kinetic energy 3.37 GeV per nucleon and nucleon–nucleon center-of-mass system (cms) energy $\sqrt{s_{nn}} = 3.14$ GeV. The QGSM is based on the Regge and string phenomenology of particle production in inelastic binary hadron collisions. To describe the evolution of the hadron and quark–gluon phases, a coupled system of Boltzmann-like kinetic equations was used in the model. The model accounted for the rescattering of hadrons as well as resonance production and decay processes. The time of hadron formation was taken into account in the QGSM. At nucleon–nucleon c.m. energy $\sqrt{s_{nn}} = 3.14$ GeV the masses of strings are smaller than 2 GeV, and these strings fragment predominantly ($\sim$90%) through two-particle decay channel.

EXPERIMENTAL PROCEDURES AND ANALYSIS

The experimental data analyzed in the present work were obtained using 2-m propane (C_3H_8) bubble chamber of Laboratory of High Energies of JINR (Dubna, Russia). The 2-m propane bubble chamber was placed in a magnetic field of strength 1.5 T [10, 20–26]. Three tantalum ^{181}Ta foils were also placed inside the propane bubble chamber. Thickness of each tantalum foil was 1 mm, and the separation distance between foils was 93 mm. The bubble chamber was then irradiated with beams of ^{12}C nuclei accelerated to a momentum of 4.2 GeV/c per nucleon at Dubna synchrophasotron. The ^{12}C nuclei were made to interact with the carbon nuclei and protons of the propane molecules and the tantalum ^{181}Ta foils placed in the propane bubble chamber [10]. Methods of selection of inelastic $^{12}C+^{12}C$ and $^{12}C+^{181}Ta$ collision events in this experiment were explained in detail in [10, 22, 24–26].

Threshold for detection of negative pions was 70 MeV/c for $^{12}C+^{12}C$ collisions, whereas for $^{12}C+^{181}Ta$ collisions it was 80 MeV/c. In some momentum and angular intervals, the particles could not be detected with 100% efficiency. To account for the loss of particles emitted under large angles to object plane of the camera as well as for the particles absorbed by tantalum foils, the relevant corrections were introduced [10, 24–26]. The average uncertainty in measurement of emission angle of negative pions was 0.8°. The mean relative uncertainty of momentum measurement of π^- mesons from the curvature of their tracks in propane bubble chamber was about 6%. All the negatively charged particles, except identified electrons, were considered to be π^- mesons. Admixtures of unidentified electrons and negative strange particles among π^- mesons did not exceed 5% and 1%, respectively. Statistics of the experimental data consist of 20528 and 2420 $^{12}C+^{12}C$ and $^{12}C+^{181}Ta$ minimum-bias collision events, respectively, with practically all the secondary particles detected under 4π solid angle. For sake of comparison with the experimental data, 30000 and 6000 minimum-bias $^{12}C+^{12}C$ and $^{12}C+^{181}Ta$ collision events at 4.2 A GeV/c, respectively, were simulated using the QGSM.

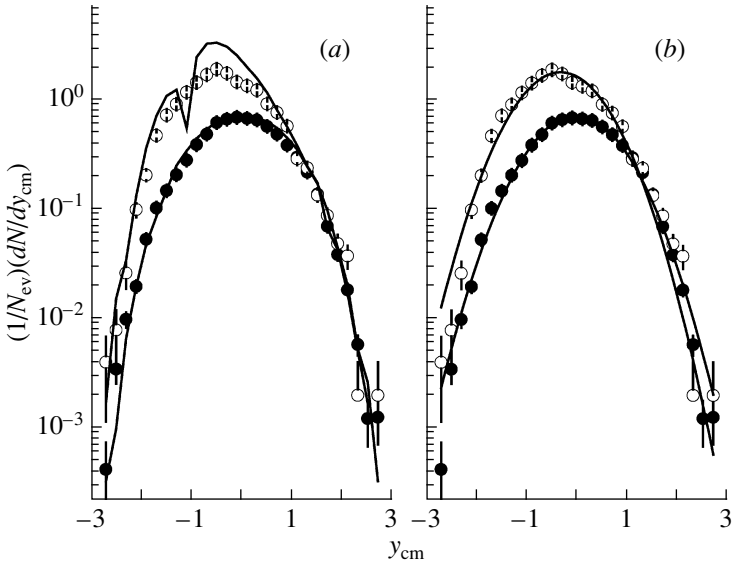

Fig. 1. The experimental rapidity distributions of negative pions in ^{12}C+^{12}C (•) and ^{12}C+^{181}Ta (○) collisions at 4.2 A GeV/c. The corresponding QGSM spectra (a) and fits by Gaussian function (b) are given by the solid curves. The spectra are obtained in cms of nucleon–nucleon collisions at 4.2 GeV/c. The distributions are normalized by the total number N_{ev} of corresponding inelastic events.

In our experiment, the spectator protons are the protons with momenta $p > 3$ GeV/c and emission angle $\theta < 4°$ (projectile spectators), and protons with momenta $p < 0.3$ GeV/c (target spectators) [10, 24–26]. The participant protons are the protons remaining after elimination of spectator protons. Comparison of the mean multiplicities per event of negative pions and participant protons and of the average values of rapidity and transverse momentum of π^- mesons in ^{12}C+^{12}C and ^{12}C+^{181}Ta collisions at 4.2 GeV/c per nucleon both in the experiment and QGSM is shown in Table 1.

Comparison of the experimental and QGSM rapidity distributions of negative pions in ^{12}C+^{12}C and ^{12}C+^{181}Ta collisions at a momentum of 4.2 GeV/c per nucleon is presented in Fig. 1a. All the spectra in Fig. 1 and the figures that follow are obtained in cms of nucleon–nucleon collisions at 4.2 GeV/c ($y_{cm} \approx 1.1$ at this incident momentum). As observed from Fig. 1a, the rapidity distribution of negative pions in ^{12}C+^{12}C collisions is symmetric with respect to midrapidity $y_{cm} = 0$, as expected for a symmetric system with identical projectile and target nuclei. It can be seen from Fig. 1a that with an increase of the target nucleus mass the height of rapidity distributions of π^- (multiplicity of π^- mesons) increases. Rapidity distribution of π^- shifts towards lower rapidity values, as is evident from Fig. 1a, or more towards target fragmentation region, as the mass of the target nucleus increases in going from ^{12}C+^{12}C to ^{12}C+^{181}Ta collisions. This is because the effective number of target participant nucleons and the number of π^- mesons produced in target fragmentation region increase as the mass of target nucleus increases. As seen from Fig. 1a, the QGSM describes satisfactorily the experimental rapidity distributions of negative pions in ^{12}C+^{12}C and ^{12}C+^{181}Ta collisions. Figure 1b shows that the experimental rapidity spectra of negative pions in ^{12}C+^{12}C and ^{12}C+^{181}Ta collisions can be fitted well by Gaussian distribution function given by

$$F(y) = \frac{A_0}{\sigma} \exp\left(\frac{-(y-y_0)^2}{2\sigma^2}\right), \qquad (1)$$

where σ is the standard deviation, referred to as a width of the distribution in the present analysis, y_0 is the centre of Gaussian distribution, and A_0 is the fitting constant. Parameters extracted from fitting the rapidity spectra of negative pions in ^{12}C+^{12}C and ^{12}C+^{181}Ta collisions at 4.2 GeV/c per nucleon by Gaussian function in Eq. (1) are given in Table 2. As seen from Table 2, the width of rapidity distribution of π^- mesons is slightly lower in ^{12}C+^{181}Ta collisions as compared to ^{12}C+^{12}C collisions both in the experiment and QGSM. The widths of experimental rapidity spectra of negative pions ($\sigma^{C+C} = 0.793 \pm 0.003$ and $\sigma^{C+Ta} = 0.75 \pm 0.01$) obtained in the present analysis proved to be slightly lower than the corresponding widths ($\sigma^{C+C} \approx 0.82$ and $\sigma^{C+Ta} \approx 0.79$) estimated in [10] for ^{12}C+^{12}C and ^{12}C+^{181}Ta collision events at 4.2 GeV/c on a significantly lower experimental statistics. It is seen from Table 2 that

Table 2. Parameters obtained from fitting the rapidity spectra of negative pions in ^{12}C+^{12}C and ^{12}C+^{181}Ta collisions at 4.2 GeV/c per nucleon by Gaussian function

Type		A_0	σ	y_0	χ^2/n.d.f.	R^2 value
^{12}C+^{12}C	Exper.	0.575 ± 0.004	0.793 ± 0.003	-0.016 ± 0.005	8.93	0.992
	QGSM	0.624 ± 0.004	0.786 ± 0.003	0.009 ± 0.005	14.21	0.983
^{12}C+^{181}Ta	Exper.	1.36 ± 0.02	0.75 ± 0.01	-0.33 ± 0.01	7.66	0.971
	QGSM	1.78 ± 0.02	0.71 ± 0.01	-0.30 ± 0.01	53.43	0.878

the locations of centers (y_0) of π^- rapidity spectra extracted from fitting by Gaussian function proved to be equal within the uncertainties to the corresponding mean rapidities of negative pions given in Table 1. As follows from Table 2, the QGSM describes satisfactorily the widths as well as the locations y_0 of rapidity distributions of negative pions in ^{12}C+^{12}C and ^{12}C+^{181}Ta collisions at 4.2 GeV/c per nucleon.

It is of interest to analyze quantitatively the change of shape of rapidity spectra of negative pions with increasing the collision centrality, which corresponds to decrease in impact parameter of collision. Since impact parameter cannot be measured directly in the experiment, we use the number of participant protons N_p to characterize the collision centrality. We follow the works [10, 27] to define the peripheral collision events as those in which $N_p \leqslant \langle n_{\text{part.prot}} \rangle$, and the central collisions as the collision events with $N_p \geqslant 2\langle n_{\text{part.prot}} \rangle$, where $\langle n_{\text{part.prot}} \rangle$ is the mean multiplicity per event of participant protons. It was shown in early work [27] that the central ^{12}C+^{181}Ta collisions at 4.2 A GeV/c selected using the above criterion were characterized by complete projectile stopping, because in these collisions the average number $\langle \nu^p \rangle$ of interacting projectile nucleons was very close to the total number of nucleons in projectile carbon. Fractions of central and peripheral ^{12}C+^{12}C and ^{12}C+^{181}Ta collision events, relative to the total inelastic cross section (σ_{in}), obtained in the present analysis for both the experimental and QGSM data are given in Table 3. As can be seen from Table 3, the experimental and corresponding model fractions of central and peripheral ^{12}C+^{12}C and ^{12}C+^{181}Ta collision events coincide with each other within two standard errors. As seen from Table 3, the central interactions constitute approximately 10% and 15% in ^{12}C+^{12}C and ^{12}C+^{181}Ta collisions, respectively, whereas the fraction of peripheral collisions is roughly 60% in both collision types. These results for ^{12}C+^{12}C and ^{12}C+^{181}Ta collisions coincide with the estimated fractions of central and peripheral collision events obtained in [10] on a significantly lower statistics of ^{12}C+^{12}C and ^{12}C+^{181}Ta collisions as compared to the statistics used in the present analysis.

Table 3. Fractions of central and peripheral ^{12}C+^{12}C and ^{12}C+^{181}Ta collisions at 4.2 GeV/c per nucleon relative to the total inelastic cross section (σ_{in})

Type	Central collisions, %		Peripheral collisions, %	
	Experiment	QGSM	Experiment	QGSM
^{12}C+^{12}C	11 ± 1	8 ± 1	58 ± 1	62 ± 1
^{12}C+^{181}Ta	16 ± 1	15 ± 1	60 ± 2	56 ± 1

In Figs. 2 and 3 the rapidity distributions of negative pions are compared for central and peripheral ^{12}C+^{12}C and ^{12}C+^{181}Ta collision events in the experiment and QGSM, respectively. All the spectra in Figs. 2 and 3 were fitted by Gaussian function given in relation (1). The corresponding parameters obtained from fitting the experimental and QGSM spectra for central and peripheral collisions are given in Table 4. As can be seen from Figs. 2 and 3 and Table 4, on the whole, all the spectra are fitted quite satisfactorily by Gaussian function. However, as seen from χ^2/n.d.f. and R^2 values, the experimental rapidity spectra are fitted significantly better by Gaussian function as compared to the QGSM spectra. As follows from Table 4, the widths of the experimental rapidity spectra of negative pions decrease by $(5 \pm 1)\%$ and $(16 \pm 2)\%$ in going from the peripheral to central ^{12}C+^{12}C and ^{12}C+^{181}Ta collisions, respectively. The similar decrease in the estimated widths of the rapidity spectra of negative pions was observed in [10] while going from the peripheral to central ^{12}C+^{12}C and ^{12}C+^{181}Ta collisions at 4.2 A GeV/c. The widths estimated for the peripheral and central ^{12}C+^{12}C and ^{12}C+^{181}Ta collisions ($\sigma^{\text{C+C}}_{\text{periph}} \approx 0.85$ and $\sigma^{\text{C+C}}_{\text{centr}} \approx$

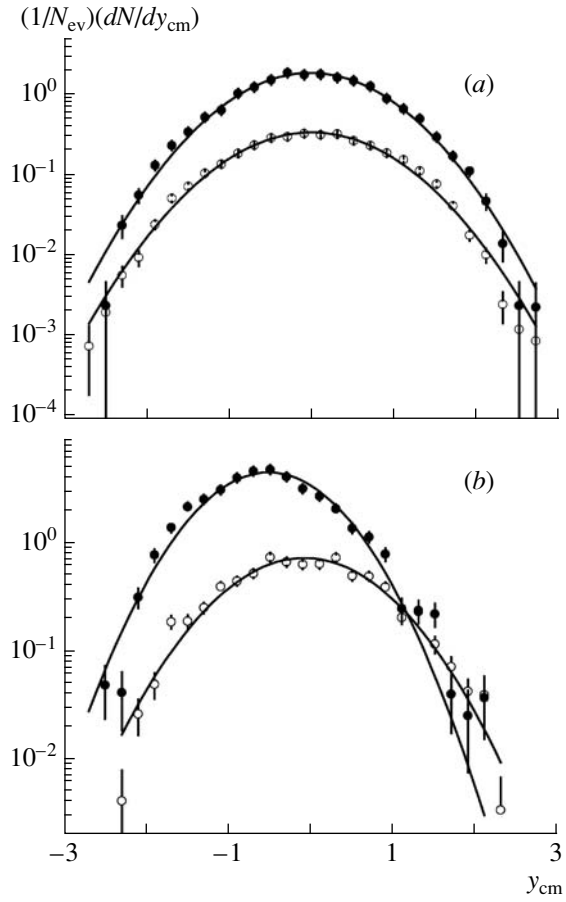

Fig. 2. The experimental rapidity distributions of negative pions in central (•) and peripheral (○) collision events in $^{12}C+^{12}C$ (*a*) and $^{12}C+^{181}Ta$ (*b*) collisions at 4.2 *A* GeV/*c*. The corresponding fits by Gaussian function are given by the solid curves. The spectra are obtained in cms of nucleon–nucleon collisions at 4.2 GeV/*c*.

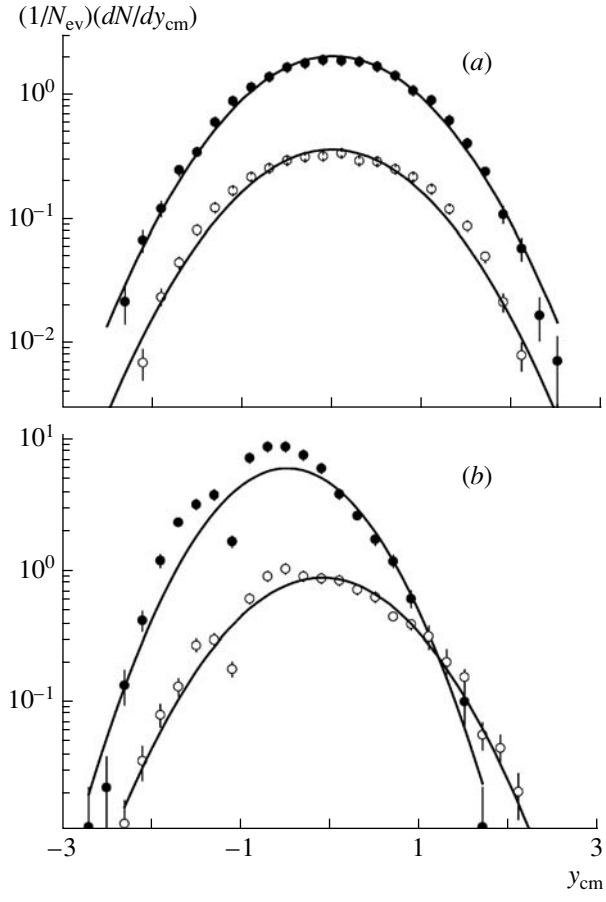

Fig. 3. Rapidity distributions of negative pions calculated using QGSM in central (•) and peripheral (○) collision events in $^{12}C+^{12}C$ (*a*) and $^{12}C+^{181}Ta$ (*b*) collisions at 4.2 *A* GeV/*c*. The corresponding fits by Gaussian function are given by the solid curves. The spectra are obtained in cms of nucleon–nucleon collisions at 4.2 GeV/*c*.

0.78, $\sigma^{C+Ta}_{periph} \approx 0.87$ and $\sigma^{C+Ta}_{centr} \approx 0.74$) in [10] proved to be slightly larger as compared to the corresponding widths of the experimental rapidity spectra shown in Table 4. The σ values obtained in the present analysis agree with the results of the early work [28], where the width of pseudorapidity distribution for shower particles varied from 0.74 for most central to 0.94 for most peripheral collisions. As seen from Fig. 2*b* and Table 4, the center y_0 of rapidity distribution of π^- mesons shifts towards target fragmentation region by -0.44 ± 0.02 units while going from peripheral to central $^{12}C+^{181}Ta$ collisions. In case of corresponding QGSM spectra, as seen from Fig. 3*b* and Table 4, the center of rapidity distribution of negative pions also shifts towards target fragmentation region by -0.39 ± 0.02 units in going from peripheral to central $^{12}C+^{181}Ta$ collisions. Such shift of peak of rapidity spectrum of π^- mesons in $^{12}C+^{181}Ta$ collisions is caused by an increase of rescattering effects in target nucleus, which is much heavier than the projectile nucleus. As a result of this, the numbers of target participant nucleons and pions produced in target fragmentation region increase substantially with increasing the collision centrality. As seen from Figs. 2*a* and 3*a* and Table 4, we do not observe such shift with increasing the collision centrality in case of rapidity spectra of negative pions in $^{12}C+^{12}C$ collisions in both the experiment and QGSM. This is due to symmetry of the colliding $^{12}C+^{12}C$ system, in which the effective numbers of participant nucleons from target and projectile ^{12}C nuclei (and the numbers of pions produced in target and projectile

Table 4. Parameters obtained from fitting the rapidity spectra of negative pions in central and peripheral $^{12}C+^{12}C$ and $^{12}C+^{181}Ta$ collisions at 4.2 GeV/c per nucleon by Gaussian function

Type		A_0	σ	y_0	χ^2/n.d.f.	R^2 value
$^{12}C+^{12}C$	Exper.	1.44 ± 0.02	0.774 ± 0.006	-0.021 ± 0.009	2.52	0.990
Central	QGSM	1.63 ± 0.02	0.794 ± 0.006	0.009 ± 0.009	2.97	0.989
$^{12}C+^{12}C$	Exper.	0.274 ± 0.003	0.813 ± 0.006	-0.008 ± 0.009	2.76	0.991
Peripheral	QGSM	0.289 ± 0.004	0.797 ± 0.006	-0.006 ± 0.009	7.32	0.972
$^{12}C+^{181}Ta$	Exper.	3.10 ± 0.07	0.68 ± 0.01	-0.52 ± 0.01	3.63	0.958
Central	QGSM	4.02 ± 0.09	0.66 ± 0.01	-0.48 ± 0.01	21.06	0.837
$^{12}C+^{181}Ta$	Exper.	0.59 ± 0.01	0.81 ± 0.01	-0.08 ± 0.02	2.82	0.967
Peripheral	QGSM	0.70 ± 0.01	0.78 ± 0.01	-0.09 ± 0.02	7.19	0.937

fragmentation regions) remain practically the same in both central and peripheral collisions. Therefore in $^{12}C+^{12}C$ collisions the rapidity distribution of negative pions remains symmetric around $y_{cm} = 0$ with increase in the collision centrality. As observed from Figs. 2 and 3 and Table 4, the center y_0 of rapidity spectra of π^- mesons in peripheral $^{12}C+^{181}Ta$ collisions proved to be close to $y_{cm} = 0$. This can be due to that in case of peripheral collisions the effective volumes of interacting regions in both the target and projectile nuclei (and thus the corresponding numbers of interacting nucleons) are close to each other.

Figure 4*a* shows the comparison of dependences of the experimental mean transverse momenta of negative pions on their nucleon–nucleon cms rapidities in $^{12}C+^{12}C$ and $^{12}C+^{181}Ta$ collisions at 4.2 GeV/c per nucleon. It is observed from Fig. 4*a* that high-p_t π^- mesons are produced in central rapidity region, whereas projectile and target fragmentation regions are occupied by the low-p_t negative pions. It can be seen from Fig. 4*a* that the height of peak of $\langle p_t \rangle$-versus-rapidity spectrum decreases with an increase of the target nucleus mass. As seen from Fig. 4*a*, the values of mean transverse momenta of π^- mesons are smaller in target fragmentation region $y_{cm} < 0$ in $^{12}C+^{181}Ta$ collisions as compared to $^{12}C+^{12}C$ collisions. This is because in case of $^{12}C+^{181}Ta$ collisions the projectile nucleons have to undergo more collisions (interactions) with more nucleons of heavy ^{181}Ta target as compared to $^{12}C+^{12}C$ collisions at the same incident momentum per nucleon. Therefore the energy transferred during the collision is shared among the greater number of participant nucleons (and the larger number of produced pions) in case of $^{12}C+^{181}Ta$ collisions as compared to $^{12}C+^{12}C$ collisions.

The corresponding to Fig. 4*a* dependences calculated using QGSM are presented in Fig. 4*b*. As seen from Fig. 4*b*, the model spectra describe quite well the behavior of the corresponding experimental spectra given in Fig. 4*a*. As can be seen from Fig. 4*b*, the height of peak of the model spectrum as well as the values of $\langle p_t \rangle$ in target fragmentation region $y_{cm} < 0$ are smaller in case of $^{12}C+^{181}Ta$ collisions as compared to $^{12}C+^{12}C$ collisions. The similar behavior was observed for the experimental spectra given in Fig. 4*a*.

The experimental $\langle p_t \rangle$-versus-y_{cm} spectra of negative pions in $^{12}C+^{12}C$ and $^{12}C+^{181}Ta$ collisions at 4.2 A GeV/c along with the corresponding fits by Gaussian function are presented in Figs. 4*c* and 4*d*. The corresponding parameters obtained from fitting the $\langle p_t \rangle$-versus-y_{cm} spectra of negative pions in $^{12}C+^{12}C$ and $^{12}C+^{181}Ta$ collisions at 4.2 GeV/c per nucleon by Gaussian function in Eq. (1) are presented in Table 5. As observed from Figs. 4*c* and 4*d* and Table 5, all the spectra are fitted quite well by Gaussian function. The values of extracted widths, as seen from Table 5, are compatible with each other and with the corresponding QGSM results in

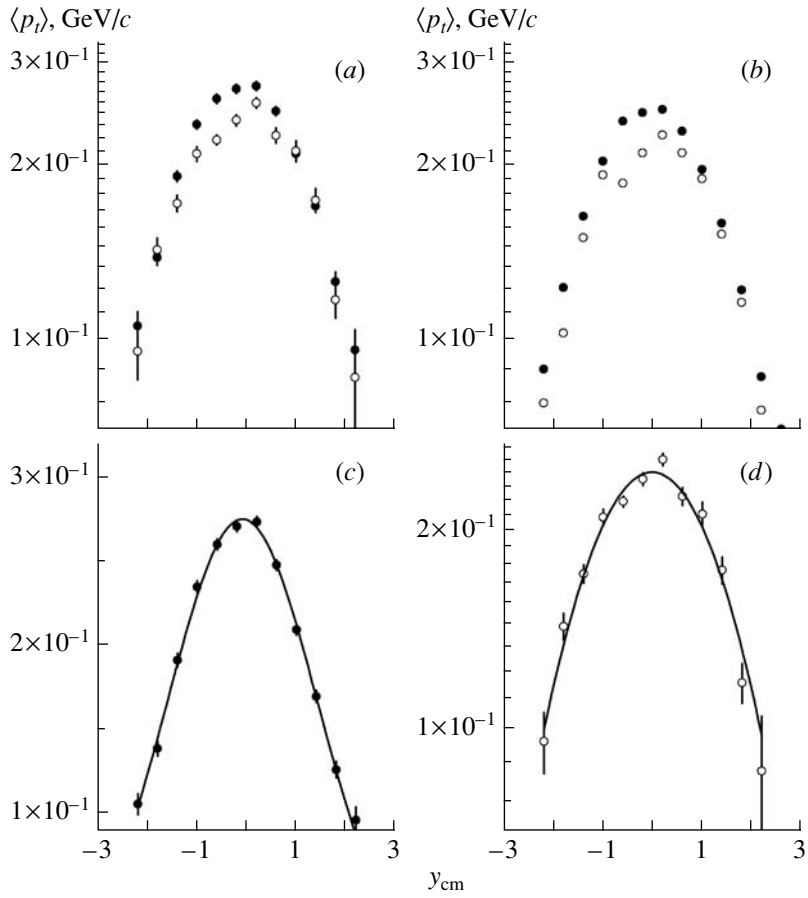

Fig. 4. (*a*) The experimental ⟨p_t⟩-versus-rapidity spectra of negative pions in $^{12}C+^{12}C$ (•) and $^{12}C+^{181}Ta$ (○) collisions at 4.2 *A* GeV/*c*; (*b*) The same as in (*a*) for QGSM spectra; (*c*) The experimental ⟨p_t⟩-versus-rapidity spectra of negative pions in $^{12}C+^{12}C$ (•) collisions at 4.2 *A* GeV/*c* along with the corresponding fit (solid curve) by Gaussian function; (*d*) The experimental ⟨p_t⟩-versus-rapidity spectra of negative pions in $^{12}C+^{181}Ta$ (○) collisions at 4.2 *A* GeV/*c* along with the corresponding fit (solid curve) by Gaussian function. All the spectra are obtained in cms of nucleon–nucleon collisions at 4.2 GeV/*c*.

$^{12}C+^{12}C$ and $^{12}C+^{181}Ta$ collisions. It is also seen that the centers y_0 of ⟨p_t⟩-versus-y_{cm} spectra of negative pions in $^{12}C+^{12}C$ and $^{12}C+^{181}Ta$ collisions are located very close to midrapidity $y_{cm} = 0$ and do not depend on the mass of target nucleus.

Furthermore we analyzed the dependences of ⟨p_t⟩-versus-y_{cm} spectra of negative pions in $^{12}C+^{12}C$ and $^{12}C+^{181}Ta$ collisions on the collision centrality. The experimental ⟨p_t⟩-versus-y_{cm} spectra of negative pions in central and peripheral $^{12}C+^{12}C$ and $^{12}C+^{181}Ta$ collisions at 4.2 *A* GeV/*c* along with the corresponding fits by Gaussian function are presented in Fig. 5. The corresponding parameters extracted from fitting the ⟨p_t⟩-versus-y_{cm} spectra of negative pions in central and peripheral $^{12}C+^{12}C$ and $^{12}C+^{181}Ta$ collisions at 4.2 GeV/*c* per nucleon by Gaussian function in the experiment and QGSM are displayed in Table 6. As observed from Fig. 5, all the spectra are described satisfactorily by Gaussian function. For both collision types, as seen from Fig. 5, the corresponding spectra coincide within the uncertainties for central and peripheral collisions. Table 6 shows that the widths extracted for the central and peripheral $^{12}C+^{12}C$ and $^{12}C+^{181}Ta$ collisions are compatible within the uncertainties with each other and with the corresponding QGSM results. As seen from Table 6, the locations of centers y_0 of ⟨p_t⟩-versus-y_{cm} spectra of negative pions in the central and peripheral $^{12}C+^{12}C$ and $^{12}C+^{181}Ta$ collisions are very close to $y_{cm} = 0$ and do not depend within the uncertainties on the collision centrality.

SUMMARY AND CONCLUSIONS

The experimental rapidity as well as ⟨p_t⟩-versus-y_{cm} spectra of negative pions in $^{12}C+^{12}C$ and $^{12}C+^{181}Ta$ collisions at a momentum of 4.2 GeV/*c*

Table 5. Parameters obtained from fitting the $\langle p_t \rangle$-versus-y_{cm} spectra of negative pions in $^{12}C+^{12}C$ and $^{12}C+^{181}Ta$ collisions at 4.2 GeV/c per nucleon by Gaussian function

Type		A_0	σ	y_0	χ^2/n.d.f.	R^2 value
$^{12}C+^{12}C$	Exper.	0.416 ± 0.004	1.51 ± 0.02	-0.09 ± 0.01	1.05	0.996
	QGSM	0.376 ± 0.003	1.50 ± 0.02	-0.03 ± 0.01	0.79	0.998
$^{12}C+^{181}Ta$	Exper.	0.40 ± 0.01	1.63 ± 0.04	-0.01 ± 0.03	2.09	0.967
	QGSM	0.354 ± 0.006	1.64 ± 0.03	0.08 ± 0.02	10.63	0.937

per nucleon were investigated. The experimental results were compared systematically with the corresponding spectra calculated using QGSM. The rapidity as well as $\langle p_t \rangle$-versus-rapidity spectra of negative pions in the analyzed collisions possessed Gaussian shape and could be fitted well by Gaussian distribution function. The locations of centers y_0 extracted from fitting the rapidity spectra of π^- mesons by Gaussian function proved to be equal within the uncertainties to the corresponding mean rapidities of negative pions in the analyzed collisions. The width (σ) of rapidity distribution of π^- mesons in $^{12}C+^{12}C$ collisions was slightly larger as compared to the corresponding σ in $^{12}C+^{181}Ta$ collisions both in the experiment and QGSM.

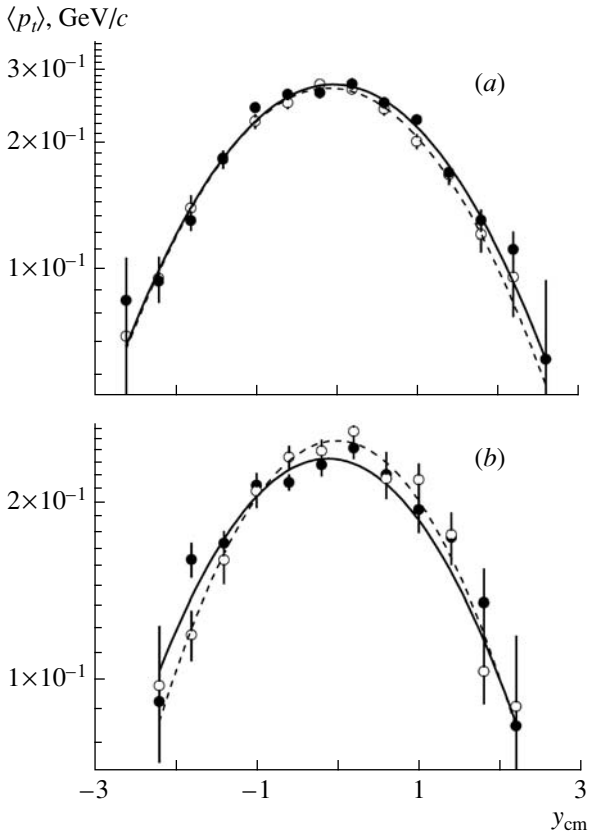

Fig. 5. The experimental $\langle p_t \rangle$-versus-rapidity spectra of negative pions in central (•) and peripheral (○) collision events in $^{12}C+^{12}C$ (*a*) and $^{12}C+^{181}Ta$ (*b*) collisions at 4.2 *A* GeV/*c*. The corresponding fits by Gaussian function for central and peripheral collisions are given by the solid and dashed curves, respectively. All the spectra are obtained in cms of nucleon–nucleon collisions at 4.2 GeV/*c*.

The widths of the experimental rapidity spectra of negative pions decreased by $(5 \pm 1)\%$ and $(16 \pm 2)\%$ in going from the peripheral to central $^{12}C+^{12}C$ and $^{12}C+^{181}Ta$ collisions, respectively. The center y_0 of experimental rapidity distribution of π^- mesons shifted towards target fragmentation region by -0.44 ± 0.02 units in going from peripheral to central $^{12}C+^{181}Ta$ collisions. This shift in y_0 of rapidity spectrum of π^- mesons in $^{12}C+^{181}Ta$ collisions could be due to increase of rescattering effects in target nucleus, which is heavier than projectile nucleus, and a subsequent increase of the numbers of target participant nucleons and pions produced in target fragmentation region with increase in the collision centrality.

The values of σ of $\langle p_t \rangle$-versus-y_{cm} spectra of negative pions in $^{12}C+^{12}C$ and $^{12}C+^{181}Ta$ collisions proved to be compatible with each other and with the corresponding QGSM results. The centers y_0 of $\langle p_t \rangle$-versus-y_{cm} spectra of negative pions in $^{12}C+^{12}C$ and $^{12}C+^{181}Ta$ collisions were located very close to midrapidity $y_{cm} = 0$ and did not depend within the uncertainties on the mass of target nucleus.

The extracted widths of $\langle p_t \rangle$-versus-y_{cm} spectra of negative pions in central and peripheral $^{12}C+^{12}C$ and $^{12}C+^{181}Ta$ collisions were compatible within the

Table 6. Parameters obtained from fitting the $\langle p_t \rangle$-versus-$y_{\rm cm}$ spectra of negative pions in central and peripheral ^{12}C+^{12}C and ^{12}C+^{181}Ta collisions at 4.2 GeV/c per nucleon by Gaussian function

Type		A_0	σ	y_0	χ^2/n.d.f.	R^2 value
^{12}C+^{12}C	Exper.	0.42 ± 0.01	1.52 ± 0.03	-0.03 ± 0.02	2.10	0.980
Central	QGSM	0.382 ± 0.005	1.54 ± 0.03	-0.04 ± 0.02	1.19	0.990
^{12}C+^{12}C	Exper.	0.40 ± 0.01	1.49 ± 0.04	-0.08 ± 0.03	0.34	0.993
Peripheral	QGSM	0.371 ± 0.005	1.48 ± 0.03	-0.02 ± 0.02	0.97	0.992
^{12}C+^{181}Ta	Exper.	0.38 ± 0.01	1.61 ± 0.04	-0.12 ± 0.04	1.68	0.987
Central	QGSM	0.34 ± 0.02	1.70 ± 0.08	0.03 ± 0.07	5.97	0.903
^{12}C+^{181}Ta	Exper.	0.38 ± 0.01	1.48 ± 0.06	-0.01 ± 0.04	1.19	0.955
Peripheral	QGSM	0.371 ± 0.005	1.48 ± 0.03	-0.02 ± 0.02	0.97	0.992

uncertainties with each other and with the corresponding QGSM results, and hence did not depend on the collision centrality. Similarly, the locations of centers y_0 of $\langle p_t \rangle$-versus-$y_{\rm cm}$ spectra of negative pions in the analyzed central and peripheral collisions were very close to $y_{\rm cm} = 0$.

We express our gratitude to the staff of Laboratory of High Energies of JINR (Dubna, Russia) and of the Laboratory of Multiple Processes of Physical–Technical Institute of Uzbek Academy of Sciences (Tashkent, Uzbekistan), who took part in the processing of stereophotographs from 2-m propane (C_3H_8) bubble chamber of JINR. We are grateful to N.S. Amelin for making available to us ^{12}C+^{12}C and ^{12}C+^{181}Ta collision events simulated using QGSM adapted to intermediate energies. Kh.K.O. is grateful to Higher Education Commission (HEC) of the Government of Pakistan for support under Foreign Faculty Hiring Program (FFHP). We thank the officials of COMSATS Institute of Information Technology (Islamabad, Pakistan) for hospitality and providing necessary facilities for the fruitful work. S.A.H. thanks the management of Karakoram International University (Gilgit-Baltistan, Pakistan), especially Vice-Chancellor and Dean of Sciences, for granting him the study leave to continue his graduate studies at Department of Physics of COMSATS Institute of Information Technology (Islamabad, Pakistan).

REFERENCES

1. D. Krpic, G. Škoro, I. Pićurić, et al., Phys. Rev. C **65**, 034909 (2002).
2. Kh. K. Olimov, Phys. Rev. C **76**, 055202 (2007).
3. Kh. K. Olimov, S. L. Lutpullaev, B. S. Yuldashev, et al., Eur. Phys. J. A **44**, 43 (2010).
4. Kh. K. Olimov, Phys. Atom. Nucl. **73**, 433 (2010).
5. Kh. K. Olimov, S. L. Lutpullaev, K. Olimov, et al., Phys. Rev. C **75**, 067901 (2007).
6. Kh. K. Olimov and Mahnaz Q. Haseeb, Eur. Phys. J. A **47**, 79 (2011).
7. Kh. K. Olimov, Mahnaz Q. Haseeb, A. K. Olimov, and Imran Khan, Centr. Eur. J. Phys. **9**, 1393 (2011).
8. Kh. K. Olimov, Mahnaz Q. Haseeb, Imran Khan, et al., Phys. Rev. C **85**, 014907 (2012).
9. Kh. K. Olimov, Mahnaz Q. Haseeb, and Imran Khan, Phys. Atom. Nucl. **75**, 479 (2012).
10. Lj. Simić, S. Backović, D. Salihagić, et al., Phys. Rev. C **52**, 356 (1995).
11. R. N. Bekmirzaev, E. N. Kladnitskaya, and S. A. Sharipova, Phys. Atom. Nucl. **58**, 58 (1995).
12. R. N. Bekmirzaev, E. N. Kladnitskaya, M. M. Muminov, and S. A. Sharipova, Phys. Atom. Nucl. **58**, 1721 (1995).
13. L. Chkhaidze, T. Djobava, L. Kharkhelauri, and M. Mosidze, Eur. Phys. J. A **1**, 299 (1998).
14. V. D. Toneev, N. S. Amelin, K. K. Gudima, and S. Yu. Sivoklokov, Nucl. Phys. A **519**, 463c (1990).
15. N. S. Amelin, K. K. Gudima, S. Yu. Sivoklokov, and V. D. Toneev, Sov. J. Nucl. Phys. **52**, 172 (1990) [Yad. Fiz. **52**, 272 (1990)]; Preprint No. P2-89-870, JINR (Dubna, 1989).

16. N. S. Amelin, K. K. Gudima, and V. D. Toneev, Sov. J. Nucl. Phys. **51**, 1093 (1990).
17. N. S. Amelin, E. F. Staubo, L. P. Csernai, et al., Phys. Rev. C **44**, 1541 (1991).
18. Kh. K. Olimov and Mahnaz Q. Haseeb, Phys. Atom. Nucl. **76**, 595 (2013) [Yad. Fiz. **76**, 638 (2013)].
19. Kh. K. Olimov, Mahnaz Q. Haseeb, and Sayyed A. Hadi, Int. J. Mod. Phys. E **22**, 1350020 (2013).
20. A. I. Bondarenko *et al.*, Phys. Atom. Nucl. **65**, 90 (2002) [Yad. Fiz. **65**, 95 (2002)].
21. L. Chkhaidze, T. Djobava and L. Kharkhelauri, Bull. Georg. Natl. Acad. Sci. **6**, 44 (2012).
22. K. Olimov, S. L. Lutpullaev, A. K. Olimov, et al., Phys. Atom. Nucl. **73**, 1847 (2010) [Yad. Fiz. **73**, 1899 (2010)].
23. L. Chkhaidze, P. Danielewicz, T. Djobava, et al., Nucl. Phys. A **794**, 115 (2007).
24. G. N. Agakishiyev *et al.*, Z. Phys. C **27**, 177 (1985).
25. D. Armutlisky *et al.*, Z. Phys. A **328**, 455 (1987).
26. A. I. Bondarenko et al., JINR Preprint No. P1-98-292, JINR (Dubna, 1998).
27. S. Backovic, V. Boldea, V. G. Grishin, et al., Sov. J. Nucl. Phys. **50**, 1001 (1989) [Yad. Fiz. **50**, 1613 (1989)].
28. EMU01 Collab. (M. I. Adamovich et al.), Phys. Rev. Lett. **69**, 745 (1992).